JOURNAL OF MATERIALS SCIENCE **34** (1999) 2441 – 2447

Electrolytic TiO_2-RuO_2 deposits

I. ZHITOMIRSKY
Israel Institute of Metals, Technion-Israel Institute of Technology, Haifa, 32000 Israel
E-mail: zhitom@mcmail.cis.McMaster.CA

Cathodic electrodeposition of RuO_2-TiO_2 coatings on Pt and Ti substrates was performed via hydrolysis by electrogenerated base of $TiCl_4$ and $RuCl_3$ salts dissolved in mixed methyl alcohol-water solvent in presence of hydrogen peroxide. The deposits were characterized by X-ray diffraction, electron microscopy, thermogravimetric and differential thermal analyses. The effect of thermal treatment on the phase content and morphology of the obtained deposits has been studied. A possible mechanism of electrodeposition is discussed.

1. Introduction

Materials in the RuO_2-TiO_2 system are of considerable interest for electrochemical, catalytic and electronic applications [1–13]. The importance of RuO_2-TiO_2 thin films, coatings, powders and aerogels for various applications has motivated the further development of processing technologies [2–4, 6, 7, 9, 10]. A cathodic electrodeposition has recently enabled the formation of different ceramic materials in the form of thin films or powders [14–18]. Electrodeposition offers advantages such as rigid control of film thickness, uniformity and deposition rate. This method is especially attractive owing to low cost of equipment and starting materials and possibility of deposition on substrates of complex shape [15, 18].

Formation of oxide materials via corresponding hydroxides or peroxides constitute two different chemical routes in cathodic electrodeposition [18–20]. In the cathodic electrodeposition process, metal ions can be hydrolyzed by an electrogenerated base to form hydroxide films on the cathodic substrate [14, 16, 18]. Oxide films were obtained by thermal dehydration of hydroxides [18, 19]. The possibility of electrodeposition of ruthenium oxide via the cathodic process was demonstrated [20, 21] on various substrates starting from aqueous $RuCl_3$ solutions. It was supposed that ruthenium species precipitate as ruthenic hydroxide or hydrated ruthenic oxide [20]. Peroxoprecursor route was designed [22] in order to solve problems associated with the electrodeposition of titania from aqueous and mixed solutions. Deposition of titania was achieved via hydrolysis of the peroxocomplex by electrogenerated base and thermal decomposition of the obtained deposit [15, 22, 23]. This approach has been further expanded to formation of other individual oxides [19] and complex compounds [17, 24]. Recent studies have demonstrated the feasibility of co-deposition of RuO_2 and TiO_2 [20]. RuO_2-TiO_2 deposits of various compositions were obtained. It is apparent [20] that electrodeposition is a very promising method for the fabrication of these composites for various applications. However, the exact mechanism of RuO_2-TiO_2 electrodeposition is not fully understood. The purpose of this work is to perform electrosynthesis of RuO_2-TiO_2 films on Pt and Ti substrates and to get a better understanding of the mechanism of deposition. The results presented involve the examination of the microstructure, composition and crystallization behavior of RuO_2-TiO_2 deposits.

2. Experimental procedures

As starting materials commercially guaranteed salts of $TiCl_4$(Merck), $RuCl_3 \cdot nH_2O$ (Fluka Chemie AG) and hydrogen peroxide H_2O_2 (30 wt % in water, Carlo Erba Reagenti) were used. The following stock solutions were prepared: (A) 0.005M $TiCl_4$ and 0.01M H_2O_2 in methyl alcohol solvent; (B) 0.005M $RuCl_3 \cdot nH_2O$ in water; (C) A and B mixed in a volume ratio A : B = 9 : 1; (D) A and B mixed in a volume ratio A : B = 3 : 1. Solutions A, C and D were prepared at 1 °C.

Rectangular Pt ($40 \times 20 \times 0.1$ mm) and Ti ($30 \times 20 \times 1$ mm) specimens were used as cathodic substrates. The electrochemical cell for deposition in a galvanostatic regime included the cathodic substrate centered between two parallel platinum counterelectrodes. Electrodeposition experiments were performed at 1 °C. Cathodic deposits were obtained at a constant current density of 20 mA/cm^2. Deposition times were in the range of up to 10 min. Multilayer deposition was performed in order to decrease cracking attributed to drying shrinkage. The obtained deposits were washed with water in order to prevent Cl impurity from the solution and dried in air. Thermal analysis was carried out in air between room temperature and 800 °C at a heating rate of 10 °C/min using a thermoanalyzer (Setaram, TGA92). X-ray diffraction patterns were recorded using a diffractometer (Phillips, PW-1820, CuK_α radiation). For the X-ray studies the deposits were annealed in air for 1 h at various temperatures. The microstructure and composition of the deposits were studied using a scanning electron microscope (Jeol, JSM-840) equipped with Energy Dispersive Spectroscopy (EDS).

3. Experimental results

Electrodeposition experiments were performed from solutions C and D and cathodic deposits (coatings C and D, respectively) were obtained. The deposits of various thickness (up to several μm) were obtained as monolayers or multilayers. Thick deposits were removed from the Pt substrates for preparation of powder samples (powders C and D, respectively). X-ray diffractograms of fresh powders and those thermally treated at 200 and 300 °C for 1 h exhibit their amorphous nature (Figs 1 and 2). Crystallization was observed at higher temperatures. XRD spectra taken from powders C (Fig. 1) after thermal treatment at 400 °C displayed reflexes of rutile and anatase. X-ray diffraction patterns for powders D exhibit only peaks of rutile (Fig. 2). The reflexes of rutile are relatively broad at 400 °C and exhibit split at 600 and 700 °C (Figs 1 and 2). Note that in this work as well as in previous experiments [20] no peaks of metallic ruthenium were observed. Fig. 3 shows XRD data for coatings C and D on Ti substrates. X-ray diffraction patterns at 450 °C show peaks of rutile and anatase in addition to those of Ti.

Fig. 4 shows an assemblage of TG/DTA curves for powders C and D. For powders C the total weight loss in temperature region up to 800 °C was about 25.1% of the initial sample weight, however essentially most of the weight loss occurred below 200 °C. The TGA curve exhibits a broad endotherm around 140 °C and an exothermic peak at 440 °C. A faint exothermic

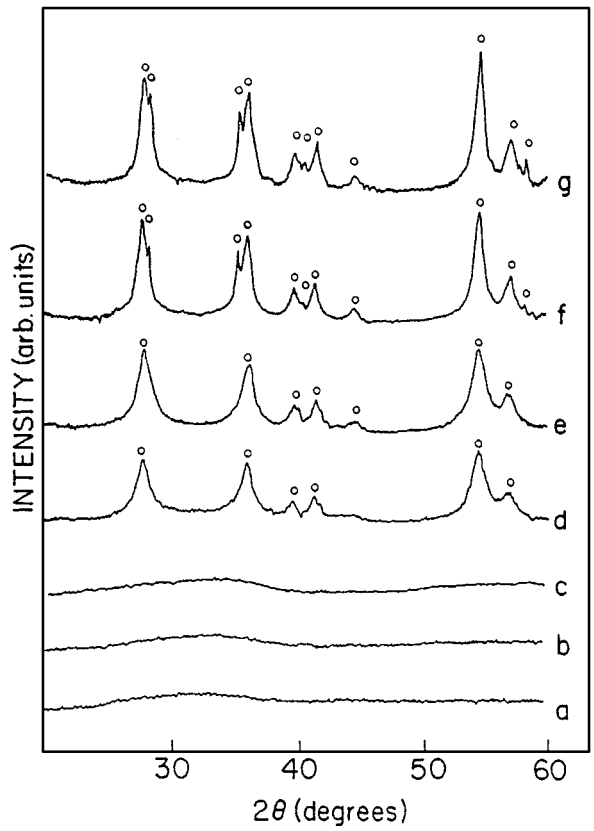

Figure 2 X-ray diffraction patterns of powders D: as prepared (a) and after thermal treatment at different temperatures for 1 h: 200 (b), 300 (c), 400 (d), 500 (e), 600 (f), and 700 °C (g) (○, rutile).

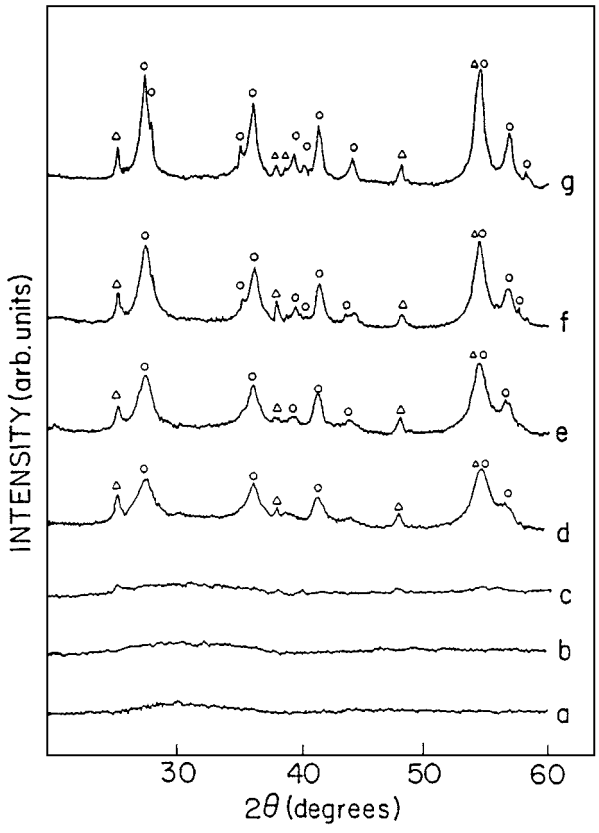

Figure 1 X-ray diffraction patterns of powders C: as prepared (a) and after thermal treatment at different temperatures for 1 h: 200 (b), 300 (c), 400 (d), 500 (e), 600 (f), and 700 °C (g) (Δ, anatase; ○, rutile).

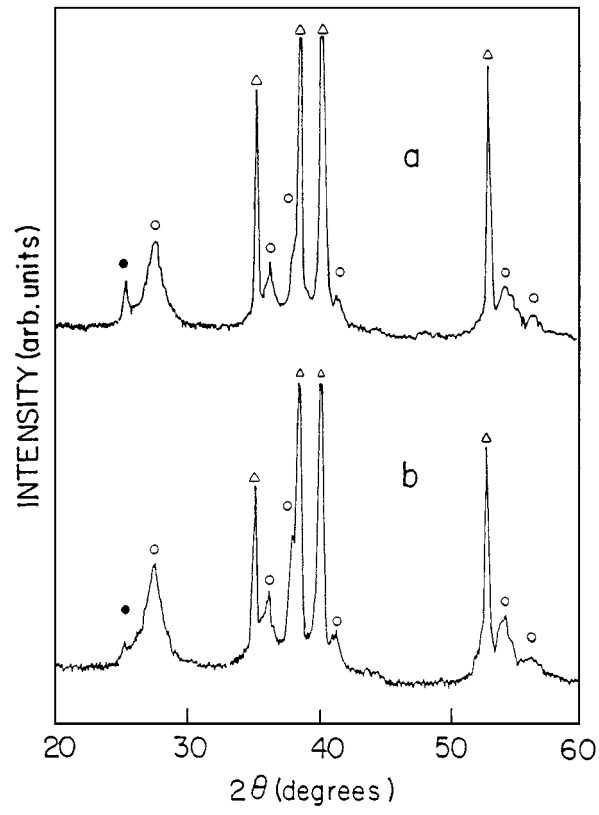

Figure 3 X-ray diffraction patterns of coatings C (a) and D (b) on Ti substrates after thermal treatment at 450 °C for 1 h (●, anatase; ○, rutile; Δ, Ti).

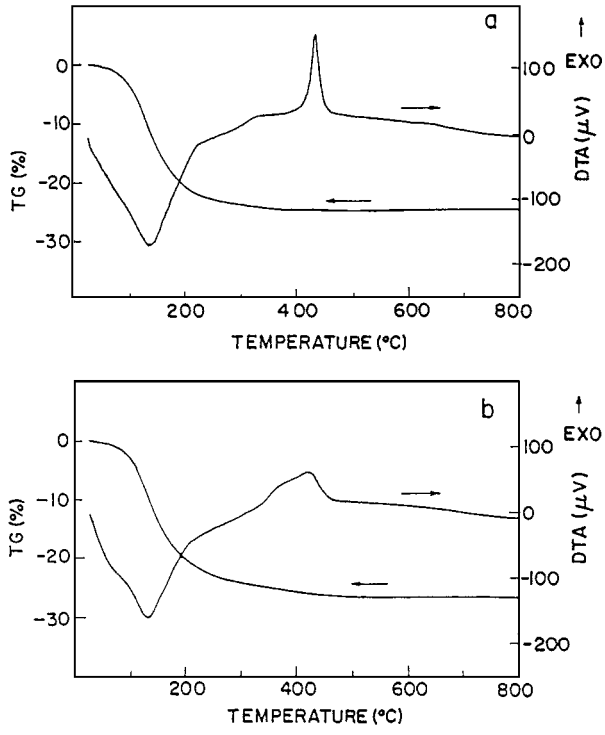

Figure 4 TG and DTA data for powders C (a) and powders D (b) obtained at a 10 °C/min heating rate.

effect was also recorded at ∼320 °C. A sharp reduction of sample weight was observed for powders D up to ∼200 °C, then the weight fell gradually. The total weight loss in the temperature region up to 800 °C was 26.6%. An endothermic effect around ∼130 °C is seen in the DTA curve for powders D. When the specimen was heated to higher temperatures a very broad exotherm around ∼400 °C was observed.

EDS spectra for powders C and D are shown in Fig. 5. Numerous EDS analyses showed a Ti/Ru ratio of 10.4 ± 0.4 for powders C and a Ti/Ru ratio of 1.7 ± 0.2 for powders D. Obtained Ti/Ru ratios in the powders differ from corresponding values in solutions due to different deposition rates of individual components.

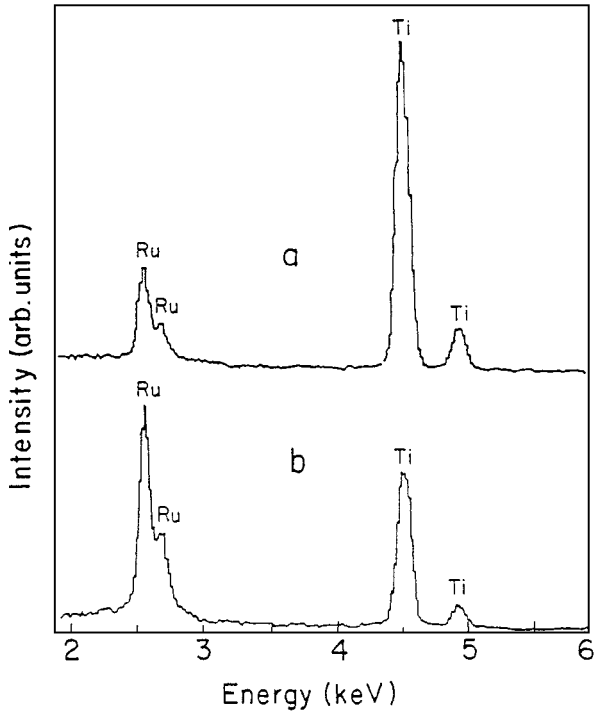

Figure 5 EDS data for powders C (a) and powders D (b).

Obtained coatings and powders were submitted to SEM examination. SEM observations of the green deposits indicated the existence of a smooth surface and very fine particle size. A continuous increase in the coating thickness with deposition time was observed. Thin deposits were crack free and adhered well to the substrates. However, deposited films were invariably cracked when their thickness exceeded ∼ 0.2–0.3 μm. This type of microcracking was related to drying shrinkage. Film sintering resulted in additional cracking. Thick deposits were obtained by multiple deposition with expectation that problems attributed to deposit cracking can be diminished. Electron microscopy shows that powders C and D (Fig. 6) thermally treated at 700 °C contain platelets of various sizes (up to 100 μm). These platelets were of uniform thickness in the range of up to 10 μm. The thickness of the platelets can be controlled by variation of deposition time. Sintered coatings exhibited a "cracked-mud" morphology when their thickness exceeded ∼1 μm. Fig. 7 shows coatings C and D on Pt substrates obtained by multiple deposition (deposition time of 20 s for each layer) and thermally treated at 600 °C. The ultrafine size of the deposit particles is noteworthy, and far below the micrometer scale. According to SEM evaluations the thickness of the deposits is about 5 μm. Currently, studies are underway to improve the deposit morphology.

4. Discussion

An important point to be discussed is the electrochemical mechanism of deposit formation. It is believed that the peroxocomplex of titanium $[Ti(O_2)(OH)_{n-2}]^{(4-n)+}$ [25] forms in solution A. Notice that ruthenium is catalytic in the decomposition reaction of H_2O_2. Therefore, after mixing of solutions A and C Ru species bring about decomposition of H_2O_2 excess. The following cathodic reactions can be considered [24]:

$$O_2 + 2H_2O + 4e^- \Leftrightarrow 4OH^- \quad (1)$$

$$2H_2O + 2e^- \Leftrightarrow H_2 + 2OH^- \quad (2)$$

Both reactions raise pH at the cathode surface.

It was suggested [20] that ruthenium and titanium species precipitate from mixed solutions as independent compounds. The high pH of the cathodic region brings about formation of a peroxotitanium hydrate $TiO_3(H_2O)_x$ [15, 22], which precipitates on the electrode. According to [4] hydrated ruthenium chloride is a heterogeneous ionic material with an average ruthenium oxidation state between 3 and 4, closer to 4. For this reason the mechanism underlying the formation of RuO_2 from the $RuCl_3 \cdot nH_2O$ precursor is complex [21]. The ruthenium species are most likely to precipitate as hydrated ruthenic oxide $RuO_2 \cdot nH_2O$ or ruthenic hydroxide $Ru(OH)_4$ [20, 26]. This process consumes electrochemically generated OH^-.

However, the mechanism of cathodic electrodeposition is not fully understood. The results described

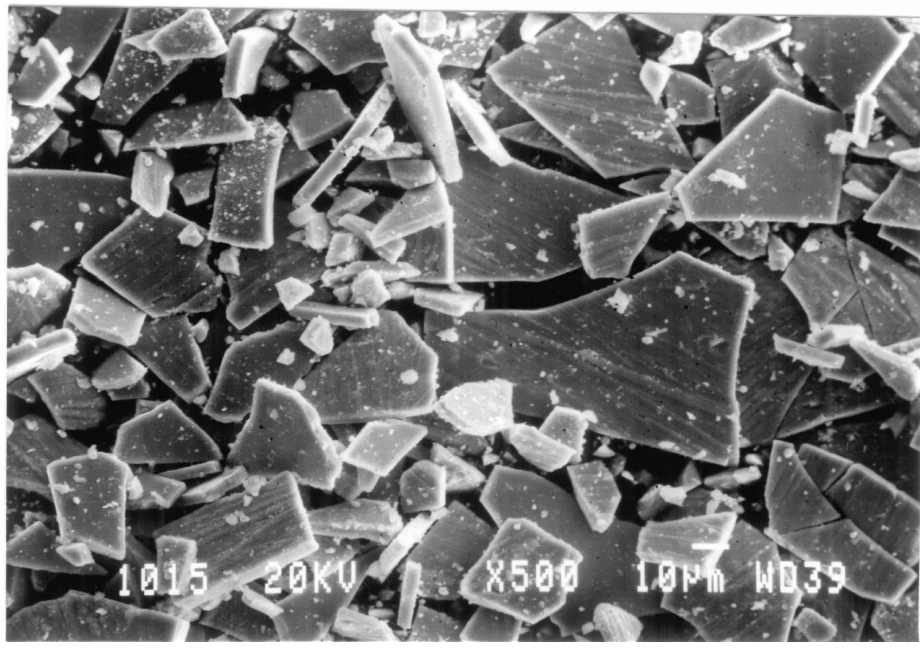

(a)

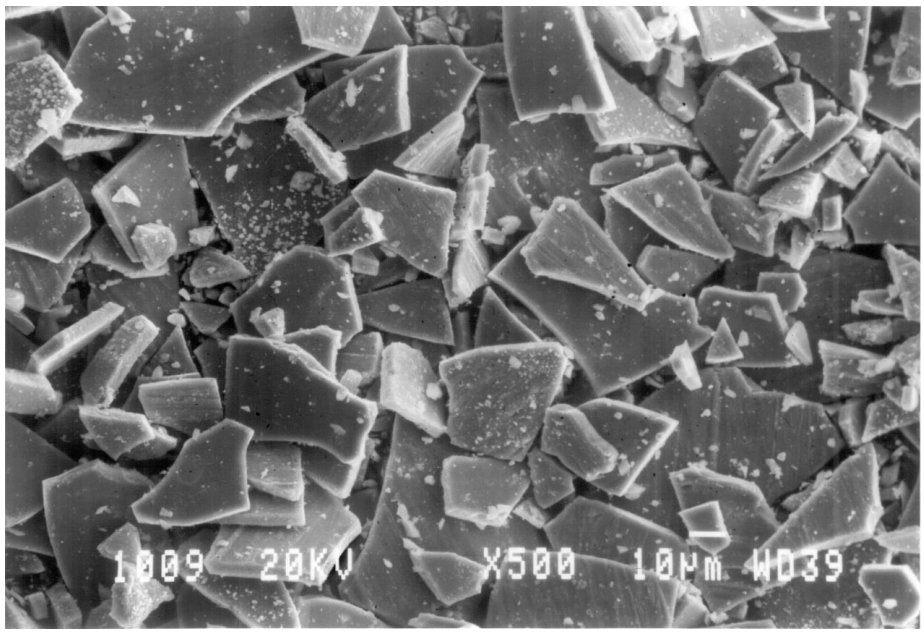

(b)

Figure 6 SEM pictures of powders C (a) and powders D (b) thermally treated at 700 °C for 1 h.

in [27] indicate that cathodic deposition of WO_3 was achieved starting from anionic tungsten-peroxide species. According to [27] a pH increase is detrimental to WO_3 deposition, as addition of NH_3 to peroxy-tungstate solution did not induce precipitation. It was suggested [27] that the peroxy-based route is completely different from deposition by a local pH increase. This concept was extended [28] to provide an explanation of the experimental data obtained in experiments on titania deposition [22]. However, proposed mechanism of deposition via the peroxy-based route [27] is not suitable to explain the results of this work. Indeed, the above experimental data show that electrodeposition of Ti and Ru species occurs simultaneously, thus allowing formation of RuO_2-TiO_2 deposits. From the preceding discussion it is seen that Ru species bring about decomposition of H_2O_2, therefore, the possibility of electrodeposition of RuO_2 via the peroxy-based route is doubtful. Moreover, in contrast to titania, electrodeposition of RuO_2 can be achieved without hydrogen peroxide [20, 21]. It is also noteworthy that the hydrous ruthenium oxide can be obtained by mixing aqueous solutions of $RuCl_3 \cdot xH_2O$ and alkalis [28]. The addition of the NaOH was used [28] for increasing the pH to a value of $\sim$7, thus allowing precipitation of RuO_2. An electrogenerated base has been utilized in previous works [20, 21] instead of alkali for the preparation of RuO_2 from an aqueous solution of $RuCl_3 \cdot xH_2O$. Note that the possibility of electrodeposition of ruthenium species by a local pH increase can be expected on the basis of the analysis of the Pourbaix equilibrium potential-pH diagram for Ru [26]. According to [25], below pH 1 the

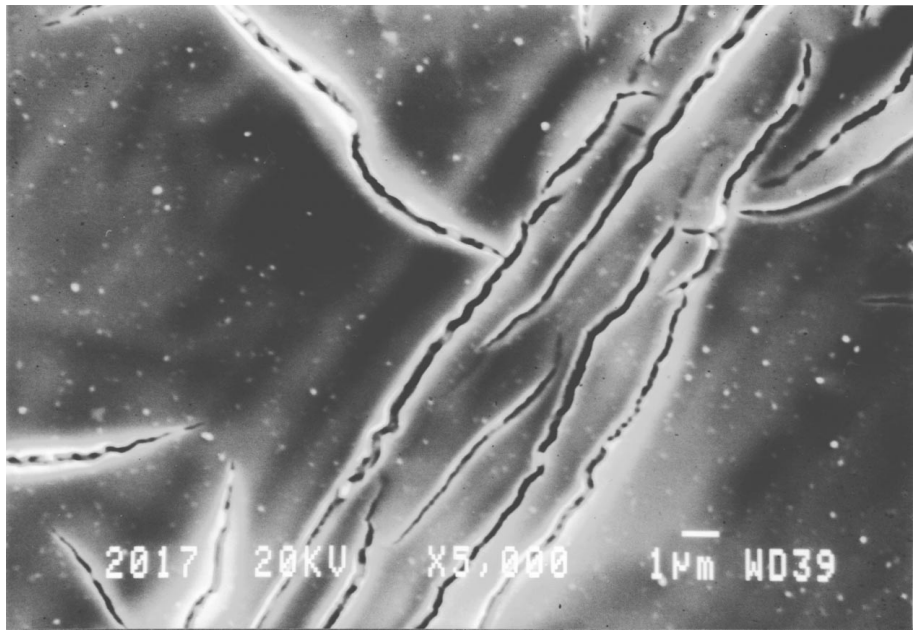

(a)

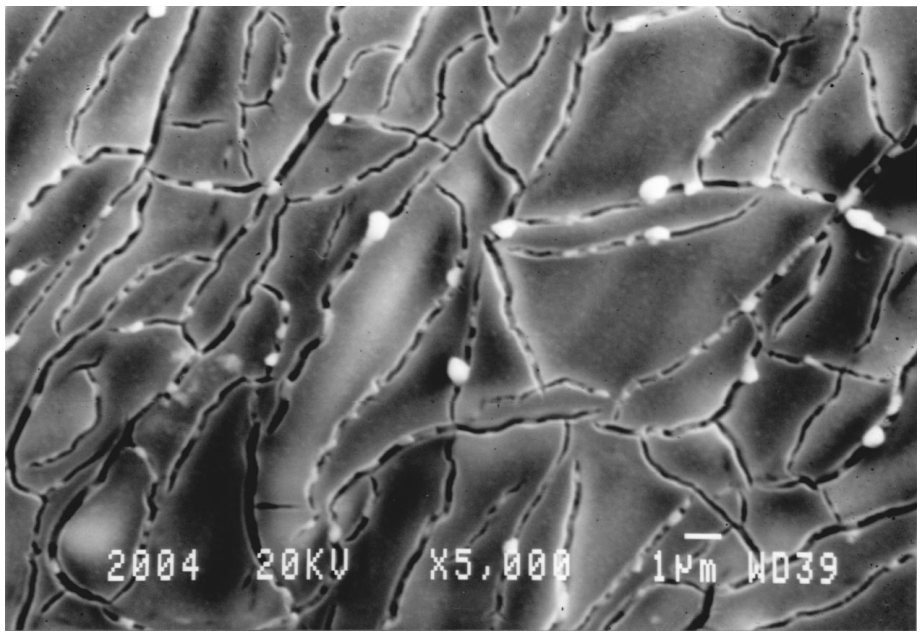

(b)

Figure 7 SEM pictures of coatings C (a) and D (b) on Pt substrates after thermal treatment at 600 °C for 1 h.

peroxocomplex of titanium $[Ti(O_2)(OH)_{n-2}]^{(4-n)+}$ is mononuclear, increase of the pH value causes transformation to a dinuclear and then to a polynuclear complex. Further pH increase results in precipitation of the peroxotitanium hydrate $TiO_3(H_2O)_x$. Turning to the experiments on powder formation formation via wet chemical methods it is seen that complex titanates can be prepared via a coprecipitation method by hydrolysis of corresponding salts with aqueous ammonia solutions [29–33]. In a series of papers [15, 17, 18, 20, 22–24, 34] it was shown that thin films and powders of titania and complex titanates can be obtained via electrosynthesis. It was pointed out that the electrosynthesis is similar to the wet chemical method of powder processing making use of electrogenerated base instead of alkali [17, 18, 34]. Therefore, results of this work coupled with previous results [15, 18, 20–24, 34] indicate that the mechanism of RuO_2-TiO_2 deposition is associated with a local pH increase.

Obtained Ti/Ru ratios in powders C and D differ from corresponding values in solutions C and D. The reason for the observed differences can be attributed to different deposition rates of individual components. According to the X-ray data, crystallization of powders C and D was observed after thermal treatment at 400 °C. Turning to the experiments on electrodeposition of individual components it should be mentioned that crystallization of RuO_2 and TiO_2 was observed at temperatures exceeding 200 and 300 °C, respectively [15, 20, 21]. TiO_2 powders and films obtained via electrodeposition possess an anatase structure up to 700 °C [15, 22, 23]. Further increase of the annealing temperature resulted in an anatase-rutile transformation. The reported results indicate, that powders C displayed XRD reflexes of

rutile and anatase at 400 °C, whereas powders D exhibit only peaks of rutile. It should be noted that RuO_2 [35] is isostructural with rutile titania [36]. Rutile is the only stable titania phase, whereas anatase [37] is metastable. It is expected that RuO_2 crystallites act as nucleation sites promoting the formation of the rutile titania phase in obtained deposits. The obtained results exhibited differences in X-ray data for powders D and coatings D. Indeed, X-ray diffraction patterns of coatings D exhibit faint peaks of the anatase phase in addition to those of rutile. It should be mentioned that peaks of anatase were also observed in RuO_2-TiO_2 coatings deposited on Ti [3], glass [3] and Pt [20] substrates. However, no formation of an anatase phase was observed in RuO_2-TiO_2 solid solutions studied in [2, 4, 5, 7]. Turning back to Figs 1–3 it should be noted that the reflexes of rutile exhibit split. This observation is in line with experimental data presented in [3, 7, 9]. It was suggested [7] that individual oxides were not completely mixed for Ti-rich compositions. It is also noteworthy that surface segregation phenomena were observed in [2, 5]. Observed split peaks were attributed to RuO_2 and TiO_2 [7, 9]. The results of Hrovat *et al.* [1] indicated the existence of solubility in the RuO_2-TiO_2 system. Therefore, split peaks can also be attributed to Ru-rich and Ti-rich solid solutions. At this point it is important to mention that one single rutile phase was observed in [4, 10]. The observed diffraction lines were attributed to the solid solution of both oxides. Following to the above considerations, it becomes evident that more detailed study, currently under way, is necessary on characterization of obtained powders and coatings.

Thermal analysis revealed weight losses for powders C and D which are attributed to a gradual decomposition of green deposits to form corresponding materials in the RuO_2-TiO_2 system. The observed endothermic peaks are associated with the weight losses. The exothermic peaks are considered to be due to crystallization of deposits and are in agreement with the X-ray data.

According to [14], insulating ceramics form very thin films. Indeed, as the coating process progresses, an insulating layer forms, which in turn prevents OH^- generation. On the other hand the uniform deposition results from the insulating properties of the deposit [18]. It is important that RuO_2 exhibits metallic conductivity [38]. Owing to significant differences in electrical resistivity of RuO_2 and TiO_2 a combination of the two materials offers an advantage in providing a desired level of coating resistivity. According to SEM observations, deposits of different thicknesses up to 10 μm were obtained. However, microscopical observations indicated development of cracks. It was pointed out [18, 21, 22] that oxide films obtained by thermal dehydration of hydroxides or peroxides exhibited cracking attributed to drying shrinkage. Note that deposit microcracking associated with drying shrinkage is a common problem in the wet chemical methods, once thick coatings are formed. In this work the cracking problem was approached by multiple deposition with expectation that cracking can be diminished in thin layers. Moreover, it was believed that deposition of the next layers will allow filling of defects which appeared after drying and annealing of previous layers. However, sintered coatings exhibited a "cracked-mud" morphology. According to [2, 12] these cracks are due to the difference in the thermal coefficient of expansion between the substrate and the coating.

Obtained results shows that electrolytic deposition is a candidate method for the preparation of RuO_2-TiO_2 coatings for dimensionally stable anodes in the chloralkali industry and other applications [1, 2, 4, 8–11]. This technique represents an alternative to dipping [2], painting [3, 10] and sol-gel [4] methods.

5. Conclusions

RuO_2-TiO_2 coatings and powders have been prepared using an electrodeposition process in solutions containing $TiCl_4$ and $RuCl_3$ salts dissolved in mixed methyl alcohol-water solvent in presence of hydrogen peroxide. RuO_2-TiO_2 coatings were obtained as monolayers or multilayers on Pt and Ti substrates. By variation of the concentration of Ru and Ti species in the starting solutions the composition of the deposited material could be controlled. The crystallization behavior and morphology of obtained deposits were studied. The deposits as-obtained were amorphous, their crystallization was observed after annealing at 400 °C. The proposed method has important advantages which make it attractive for practical applications.

References

1. M. HROVAT, J. HOLC, Z. SAMARDZIJA and G. DRAZIC, *J. Mater. Res.* **11** (1996) 727.
2. K. KAMEYAMA, K. TSUKADA, K. YAHIKOZAWA and Y. TAKASU, *J. Electrochem. Soc.* **140** (1993) 966.
3. F. HINE, M. YASUDA and T. YOSHIDA, *ibid.* **124** (1977) 500.
4. M. GUGLIELMI, P. COLOMBO, V. RIGATO, G. BATTAGLIN, A. BOSCOLO-BOSCOLETTO and A. DE BATTISTI, *ibid.* **139** (1992) 1655.
5. A. DE BATTISTI, G. LODI, M. CAPPADONIA, G. BATTAGLIN and R. KÖTZ, *ibid.* **136** (1989) 2596.
6. J. MINK, J. KRISTÓF, A. DE BATTISTI, S. DAOLIO and C. S. NÉMETH, *Surface Science* **335** (1995) 252.
7. K. KAMEYAMA, S. SHOHJI, S. ONOUE, K. NISHIMURA, K. YAHIKOZAWA and Y. TAKASU, *J. Electrochem. Soc.* **140** (1993) 1034.
8. C. E. VALLET, B. V. TILAK, R. A. ZUHR and C. P. CHEN, *ibid.* **144** (1997) 1289.
9. K. E. SWIDER, C. I. MERZBACHER, P. L. HAGANS and D. R. ROLISON, *Chem. Mater.* **9** (1997) 1248.
10. J. AUGUSTYNSKI, L. BALSENC and J. HINDEN, *J. Electrochem. Soc.* **125** (1978) 1093.
11. L. R. CZARNETZKI and L. J. J. JANSSEN, *J. Appl. Electrochemistry* **22** (1992) 315.
12. S. PUSHPAVANAM and K. C. NARASIMHAM, *J. Mater. Sci.* **29** (1994) 939.
13. Y. TAKASU, Y. MURAKAMI, S. MINOURA, H. OGAWA and K. YAHIKOZAWA, in "Proceedings of the Symposium on Electrochemical Capacitors," edited by F. M. Delnick and M. Tomkiewicz (The Electrochemical Society, Inc., Pennington, NJ, 1996) Vol. 95-29, p. 57.
14. J. A. SWITZER, *Amer. Ceram. Soc. Bull.* **66** (1987) 1521.
15. I. ZHITOMIRSKY, *NanoStructured Materials* **8** (1997) 521.
16. R. CHAIM, G. STARK, L. GAL-OR and H. BESTGEN, *J. Mater. Sci. Lett.* **13** (1994) 487.
17. I. ZHITOMIRSKY, L. GAL-OR and S. KLEIN, *ibid.* **14** (1995) 60.
18. I. ZHITOMIRSKY and L. GAL-OR, in "High Temperature Coatings," edited by N. B. Dahotre (Marcel Dekker, Inc.), in press.
19. I. ZHITOMIRSKY and L. GAL-OR, *J. Mater. Sci.*, in press.

20. *Idem., Mater. Lett.*, in press.
21. I. ZHITOMIRSKY and L. GAL-OR, *ibid.* **31** (1997) 155.
22. I. ZHITOMIRSKY, L. GAL-OR, A. KOHN and H. W. HENNICKE, *J. Mater. Sci.* **30** (1995) 5307.
23. I. ZHITOMIRSKY and L. GAL-OR, *J. Eur. Ceram. Soc.* **16** (1996) 819.
24. I. ZHITOMIRSKY, A. KOHN and L. GAL-OR, *Mater. Lett.* **25** (1995) 223.
25. J. MUHLEBACH, K. MULLER and G. SCHWARZENBACH, *Inorg. Chem.* **9** (1970) 2381.
26. M. POURBAIX, "Atlas of Electrochemical Equilibria in Aqueous Solutions" (National Association of Corrosion Engineers, Houston, Texas, 1974) p. 344.
27. E. A. MEULENKAMP, *J. Electrochem. Soc.* **144** (1997) 1664.
28. J. P. ZHENG, P. J. CYGAN and T. R. JOW, *ibid.* **142** (1995) 2699.
29. M. MURATA, K. WAKINO, K. TANAKA and Y. HAMAKAWA, *Mater. Res. Bull.* **11** (1976) 323.
30. Y. YOSHIKAWA and K. TSUZUKI, *J. Eur. Ceram. Soc.* **6** (1990) 227.
31. J. A. NAVIO, F. J. MARCHENA, M. MACIAS, P. J. SANCHEZ-SOTO and P. PICHAT, *J. Mater. Sci.* **27** (1992) 2463.
32. J.-H. CHOY, Y. S. HAN and J. T. KIM, *J. Mater. Chem.* **5** (1995) 65.
33. G. PFAFF, *Ceramics International* **20** (1994) 111.
34. I. ZHITOMIRSKY, L. GAL-OR, A. KOHN and M. D. SPANG, *J. Mater. Sci.* **32** (1997) 803.
35. JCPDS Index Card 40-1290, Joint Committee for Powder Diffraction Studies, Swarthmore, PA, 1990.
36. JCPDS Index Card 21-1276, Joint Committee for Powder Diffraction Studies, Swarthmore, PA, 1980.
37. JCPDS Index Card 21-1272, Joint Committee for Powder Diffraction Studies, Swarthmore, PA, 1980.
38. W. D. RYDEN, A. W. LAWSON and C. C. SARTAIN, *Phys. Rev. B* **1** (1970) 1494.

Received 21 October 1997
and accepted 15 October 1998